

IMPACT OF DIETARY MAGNESIUM UPON INSULIN
SENSITIVITY, VASCULAR FUNCTION, AND
METABOLIC COMPLICATIONS DURING
DEVELOPMENT OF TYPE 2 DIABETES

by

Alexander James Barker Smith

A thesis submitted to the faculty of
The University of Utah
in partial fulfillment of the requirements for the degree of

Master of Science

Department of Nutrition and Integrative Physiology

The University of Utah

December 2017

Copyright © Alexander James Barker Smith 2017

All Rights Reserved

The University of Utah Graduate School

STATEMENT OF THESIS APPROVAL

The thesis of Alexander James Barker Smith

has been approved by the following supervisory committee members:

Thunder Jalili, Chair 10/17/2017
Date Approved

John David Symons, Member 10/17/2017
Date Approved

Sihem Boudina, Member 10/17/2017
Date Approved

and by Scott Summers, Chair of
the Department of Nutrition and Integrative Physiology

and by David B. Kieda, Dean of The Graduate School.

ABSTRACT

Background: Epidemiological data associates low magnesium (Mg) intake with greater risk of metabolic syndrome/diabetes, and Mg status is often compromised in diabetic patients. It remains unclear whether low Mg consumption may exacerbate the metabolic disruptions that occur during diabetes.

Objective: We hypothesized low dietary Mg during the development of diabetes would alter metabolic rate, and worsen glucose tolerance/insulin sensitivity.

Methods: Three cohorts ($n = 8$ each) of 8-week-old TallyHo (TH) mice that develop Type 2 Diabetes by 16 weeks of age were fed special diets for 8 weeks. Group 1: TH + Low Mg diet (L-Mg, 100mg Mg Oxide/kg chow). Group 2: TH + Standard Mg diet (S-Mg, 500mg Mg Oxide/kg chow). Group 3: TH + High Mg diet (H-Mg, 1000mg Mg Bisglycinate/kg chow). Age-matched male C57BL/6J mice fed standard diets served as controls (Con, $n = 8$, 500mg Mg Oxide/kg chow).

Results: Energy expenditure was lowest ($p < 0.05$) in L-Mg vs. all other groups. Insulin tolerance test (AUC, glucose mg/dL), indicated insulin resistance ($p < 0.05$) in L-Mg (12394 ± 2344) vs. Con (3866 ± 2344), and a trend ($p = 0.052$) indicating greater insulin resistance in S-Mg (10429 ± 2193) vs. Con. However, insulin tolerance was normalized in H-Mg (7838 ± 2344) vs. Con. QUICKI index indicated that all groups were insulin resistant ($p < 0.05$) compared to Con (0.585 ± 0.14). However, L-Mg (0.403

± 0.15) had greater ($p < 0.05$) insulin resistance than S-Mg (0.462 ± 0.17) and H-Mg (0.454 ± 0.15). Insulin stimulated phosphorylation of hepatic insulin receptor was similar among all groups, whereas Akt phosphorylation was reduced ($p < 0.05$) in all diabetic mice regardless of Mg intake.

Conclusions: Low dietary Mg intake reduces oxygen consumption and energy expenditure, and worsens insulin sensitivity in diabetic mice. Supplemental Mg can partially reduce fasting glucose and improve insulin tolerance, but could not be attributed to an improvement in hepatic insulin signaling.

TABLE OF CONTENTS

ABSTRACT.....	iii
LIST OF TABLES.....	vi
LIST OF FIGURES.....	vii
ACKNOWLEDGEMENTS.....	viii
INTRODUCTION.....	1
METHODS.....	3
Animals and Diets.....	3
Overview of Experimental Procedures.....	4
Nuclear Magnetic Resonance.....	4
Comprehensive Lab Animal Monitoring System (CLAMS).....	4
Glucose and Insulin Tolerance Tests.....	5
Tissue Collection Protocol.....	5
Bone Mg Content.....	6
Vessel Function.....	6
Western Blots.....	6
Data Analysis.....	7
RESULTS.....	8
Tissue Analysis.....	8
Final Body Weight and Composition.....	8
Oxygen Consumption and Energy Expenditure.....	8
Insulin Sensitivity.....	9
Vessel Function.....	10
Western Blots.....	10
DISCUSSION.....	18
REFERENCES.....	23

LIST OF TABLES

Tables

1 Characteristics of vessels from vessel function experiments.....	11
--	----

LIST OF FIGURES

Figures

1 Bone Mg concentrations, measured in milligrams per gram, for the 3 diabetic mouse groups and the control group.....	12
2 Body composition assessment for the 3 diabetic mouse groups and the control group.....	13
3 Measurements taken using CLAMS for the 3 diabetic mouse groups and the control group.....	14
4 Insulin sensitivity measurements for the 3 diabetic mouse groups and the control group.....	15
5 Vessel function curves for the 3 diabetic mouse groups and the control group.....	16
6 Phospho-Insulin Receptor (IR), IR, Phospho-Akt, and Akt concentrations in liver tissue samples between saline and insulin-stimulated mice.....	17

ACKNOWLEDGEMENTS

I would like to thank my committee members, Dr. Thunder Jalili, Dr. John David Symons, and Dr. Sihem Boudina, for their support in completing this thesis project. I would also like to thank Jessica Challburg, Brian Duke, Andrew L. O'Farrell, Chrissy McGarry, and Robbie Barker for their help with animal care, tissue collection, and laboratory work.

INTRODUCTION

Magnesium is required as a cofactor in over 300 enzyme-catalyzed reactions (1). Magnesium functions either directly as a cofactor in the structure of enzymes, or as part of the Mg-adenosine triphosphate (ATP) complex. When Mg binds ATP, it partially shields the negative charges associated with the gamma and beta phosphoryl groups, as well as favorably altering the orientation of these phosphoryl groups (2). Mg is therefore essential for ATP hydrolysis, which is required in almost every metabolic pathway. For example, during the insulin signaling pathway, downstream phosphorylation reactions requiring Mg, such as the phosphorylation of insulin receptor and Akt, stimulate Glucose Transporter Type 4 (GLUT4) translocation to the cell membrane, resulting in glucose uptake into liver and muscle cells (2).

The Recommended Dietary Allowance (RDA) for Mg intake in American adults ranges from 310 milligrams (mg) to 420mg per day. Unfortunately, many Americans don't consume adequate dietary Mg. According to the 1999-2000 National Health and Nutrition Examination Survey (NHANES), mean daily Mg intake of the 3,510 individuals interviewed in person was 290mg (3). Median dietary intake of Mg was lower than the RDA and Estimated Average Requirement (EAR) for all groups analyzed (except for Caucasian men aged 31 to 50 years) (3). Consistently low Mg intake can increase the risk of complications in a multitude of diseases, due to alterations in various biochemical pathways. Disease examples include cardiovascular disease, hypertension,

osteoporosis, and type 2 diabetes mellitus (T2D) (1). Both low Mg status (4,5) and consumption (6) have been associated with an increased risk for developing T2D in humans. Additionally, multiple studies have shown improved metabolic parameters in animal models fed a high Mg diet, including improved fasting glucose and insulin sensitivity (7,8,9). In this context, it is possible that low Mg status may impact phosphorylation reactions required for pathways such as insulin signaling, due to the integral role of the Mg-ATP complex in phosphorylation reactions. This scenario could lead to insulin resistance, or a worsening of insulin resistance during T2D.

In our experiments, we utilized an established model of T2D, the TallyHo (TH) mouse, and compared diabetic complications in mice fed a low, normal or high Mg diets. We hypothesized that TH mice fed a low Mg diet would have greater metabolic impairments and greater insulin resistance than mice fed normal Mg diets. We also evaluated if diets high in Mg could improve parameters of metabolism or insulin signaling. We found that TH mice fed a low Mg diet have reduced energy expenditure, and further exacerbated insulin resistance and hyperglycemia.

METHODS

Animals and Diets

All protocols were approved by the University of Utah Institutional Animal Care and Use Committee. The TallyHo (TH) polygenic mouse model (Jackson Laboratories, Bar Harbor, ME) was used in this study to assess the effects of dietary Mg on T2D. As TH mice progress from 6 to 16 weeks of age, they develop multiple characteristics associated with human T2D. Adults are characterized by hyperglycemia, hyperinsulinemia, insulin resistance, and obesity (10). Quantitative trait loci (QTL) *Tanidd1*, located on mouse chromosome 19, *Tanidd2* on chromosome 13, *Tanidd3* on chromosome 15, TallyHo-associated body weight (*Tabw1*) on chromosome 7, and TallyHo-associated fat pad (*Tafat*) on chromosome 6 all contribute to the hyperglycemic phenotype of TH mice (10).

Four experimental groups were used in this study, each with an $n = 8$. The control group contained nondiabetic C57BL/6J mice (Jackson Laboratories, Bar Harbor, ME), which were fed a standard diet of 500mg Mg per kilogram (kg) of chow, the recommended Mg intake for rodents in the American Institute of Nutrition (AIN) 93-M diet. There were 3 intervention groups, which all used the TallyHo diabetic mouse model. These groups were fed a low (100mg/kg chow Mg oxide), standard, or high Mg (1000mg/kg chow Mg bisglycinate) diet. In our previous, unpublished studies, Mg bisglycinate has been shown to be the most bioavailable Mg supplement. All diets were

formulated and purchased from Research Diets (New Brunswick, NJ, USA).

Overview of Experimental Procedures

All mice began the feeding protocol at 8 weeks old. All cages were changed daily, to ensure minimal fecal consumption by mice. After completing the 8-week feeding protocol, full body metabolism was assessed using Comprehensive Lab Animal Monitoring System (CLAMS). Body composition was examined using Nuclear Magnetic Resonance (NMR). Bone Mg status was determined by assessing bone Mg content. Femoral arterial dysfunction was assessed using a wire myograph. Fasting glucose, fasting insulin, glucose tolerance and insulin tolerance were all measured. Insulin signaling in liver samples was determined by measuring total and phosphorylated levels of Insulin receptor and Akt after either insulin or saline treatment.

Nuclear Magnetic Resonance

Using a Bruker Minispec (Billerica, MA), mice were analyzed for both grams and percentage of body weight constituting from fat, lean tissue, and fluid as previously described (11).

Comprehensive Lab Animal Monitoring System (CLAMS)

Columbus Instruments Comprehensive Lab Animal Monitoring System (CLAMS, Columbus Instruments, Columbus, OH) was used to measure 3-dimensional movement, food and water consumption, heat production, oxygen consumption, and CO₂ production, during a 72-hour measuring period as previously described (11).

Glucose and Insulin Tolerance Tests

Glucose Tolerance Tests (GTT) measured glucose clearance after an intraperitoneal (IP) injection of 1 milligram (mg) glucose per gram body mass. Insulin Tolerance Tests (ITT) measured glucose clearance after an IP injection of 0.75 units insulin per kilogram body mass. Mice were fasted 6 hours prior to both GTT and ITT experiments, and housed individually with water during the experiments. All experiments started at 2:30pm.

Insulin resistance was calculated from fasting glucose and insulin concentrations using the homeostatic model assessment of insulin resistance (HOMA-IR) as described (12) using the following formula: $(\text{glucose (mg/dL)} \times \text{insulin (mU/L)}) / 22.5$. Insulin sensitivity was calculated using the quantitative insulin sensitivity check index (QUICKI) as described (13) with the following formula: $1 / \log [\text{fasting insulin (mU/mL)} + \log (\text{fasting glucose (mg/dL)})]$.

Tissue Collection Protocol

Mice were injected IP with saline or insulin (1U/kg) to stimulate activation of the insulin signaling pathway, then anesthetized using 3-5% isoflurane until the requisite plane of anesthesia was obtained. The chest cavity was opened. Cardiac puncture was performed to obtain a blood sample (750 ul-1000ul). Heart, gastrocnemius, and liver samples were taken and flash frozen in liquid N₂. Tibia and fibula were saved for later analysis of bone mineral content.

Bone Mg Content

Bone samples were dried and ashed at 500°C for 10 hours, after which the ash was dissolved in 0.2 mL concentrated HNO₃ and 9.2 mL distilled water. For total Mg determination, tissue samples were diluted appropriately with 0.1% lanthanum chloride. Mg level was then calculated using flame atomic absorption spectrometry and compared to standard curves constructed from known Mg concentrations.

Vessel Function

Femoral arteries were taken immediately following euthanizing mice, and adherent tissue was removed while immersed in ice-cold dissection buffer containing protease and phosphatase inhibitors (14). Vessels were mounted on a wire myograph (BioPac Systems, Santa Barbara, CA). The vessels completed a series of internal circumference active tension curves to determine the vessel diameter at which the greatest tension development occurred (14). Following this, the vessels were subjected to the following conditions: phenylephrine (receptor mediated contraction), potassium chloride (KCl) (nonreceptor mediated contraction), acetylcholine (endothelium-dependent vasorelaxation), and sodium nitroprusside (endothelium-independent vasorelaxation) (14). At least 30 minutes separated each protocol (14).

Western Blots

Proteins within liver samples were separated according to size, using sodium dodecyl sulfate (SDS) polyacrylamide gel electrophoresis. Using Turbo Transfer (BioRad, Hercules, CA), proteins were transferred to nitrocellulose membranes.

Membranes were blocked for one hour at room temperature, using Licor blocking buffer (Licor Biosciences, Lincoln, NE), to prevent nonspecific binding of primary and/or secondary antibodies. Membranes were then incubated with primary antibodies directed against phosphorylated and total Insulin receptor (β subunit, tyrosine 1361) and Akt (serine 473), in Licor blocking buffer overnight at 4°C (1:1000 dilution). Next, membranes were washed three times with 0.1% PBS-T, at five minutes per wash and then incubated with secondary antibody (Licor Biosciences, Lincoln, NE) at a 1:5000 dilution in Licor blocking buffer for one hour in an ultraviolet-protected container. Following 3 washes with 0.1% PBS-T, membranes were imaged using a Licor Odyssey infrared scanner (Lincoln, NE) to quantify band densities. All primary antibodies were purchased from Cell Signaling Technology (Beverly, MA).

Data Analysis

Data are reported as means +/- standard error. Data were analyzed via one-way ANOVA for all measurements, except for vessel function and Western Blots. Tukey's post hoc test was used to detect differences between groups. Vessel function was analyzed via repeated measures ANOVA. Western Blots were analyzed using ANOVA for saline-treated mice and insulin-treated mice as independent groups. Tukey's post-hoc test was then used to detect differences between groups if main effects were detected. Significance for all analyses was accepted at $p < 0.05$.

RESULTS

Tissue Analysis

All diabetic groups, especially mice fed the low Mg diet, had lower bone Mg concentrations versus mice in the control group. Additionally, there was a strong trend for TH mice fed the low Mg diet to have lower bone Mg, compared to the TH mice fed the standard ($p = 0.066$) or high ($p = 0.069$) Mg diets (**Figure 1**).

Final Body Weight and Composition

All TH mice, regardless of their diet, had significantly higher body mass, higher fat mass, and lower lean mass, compared with the control mice fed the standard diet (**Figure 2A, B, C**).

Oxygen Consumption and Energy Expenditure

Mice fed the low Mg diet had the lowest oxygen consumption, while mice fed the standard and high Mg diets had similar oxygen consumption to the control mice (**Figure 3A**). There were no significant differences observed in carbon dioxide production between any of the experimental groups (**Figure 3B**). Mice fed the low Mg diet had the highest respiratory exchange ratio, while mice fed the standard and high Mg diets were similar to the control mice (**Figure 3D**).

Mice fed the low Mg diet also had the lowest energy expenditure, while levels

were unchanged across all other groups (**Figure 3E**). Finally, mice fed the low and standard Mg diets were the most sedentary according to beam break counts, while mice fed the high Mg diet had similar physical activity levels to the control group mice (**Figure 3C**).

Insulin Sensitivity

Fasting hyperglycemia was observed in mice fed the low and standard Mg diets. Additionally, there was a partial improvement in fasting glucose in the mice fed the high Mg diet towards the control group fasting glucose concentration (**Figure 4A**). Conversely, fasting insulin levels remained high in all diabetic mouse groups, compared to the control group (**Figure 4B**). Glucose tolerance was significantly worse in all diabetic mouse groups, versus mice fed the control diet (**Figure 4C**). Insulin tolerance was significantly worse in mice fed the low and standard Mg diet, indicating insulin resistance. There was also a partial recovery of insulin tolerance in mice fed the high Mg diet bringing it more in line with the control group level (**Figure 4D**).

All diabetic mouse groups had lower insulin sensitivity as calculated by QUICKI index versus the control group (**Figure 4E**). Mice on the low Mg diet were found to have the least insulin sensitivity. Insulin resistance was estimated using HOMA-IR index, and mice fed the low and high Mg diets had greater insulin resistance than controls, while the standard Mg diet group was similar to both the high Mg and the control groups (**Figure 4F**). Again, mice fed the low Mg diet were the most insulin resistant.

Vessel Function

All vessel characteristics were nonsignificant. (**Table 1**). No difference was noted between any of the femoral arteries when assessing endothelium-dependent vasorelaxation (**Figure 5A**), endothelium-independent vasorelaxation (**Figure 5B**), or receptor-mediated vasoconstriction (**Figure 5C**). A significantly greater nonreceptor mediated contraction was seen in the femoral arteries of the control group versus all three diabetic groups, at concentrations of 60, 80, and 100 millimolar KCl (**Figure 5D**).

Western Blots

Insulin-stimulated phosphorylation of IR was similar across all groups (**Figure 6**). Insulin-stimulated phosphorylation of Akt was significantly blunted in all TH mice groups, compared to normal phosphorylation events occurring in control mice (**Figure 6**).

Table 1. Characteristics of vessels from vessel function experiments.

	Start Width (μm)	End Width (μm)	Vessel Length (μm)	PE % change
TH 100 MgO	165.6 +/- 8.1	493.8 +/- 7.8	1975.0 +/- 18.9	0.69 +/- 0.05
TH 500 MgO	181.3 +/- 10.3	478.1 +/- 8.8	1906.3 +/- 41.7	0.65 +/- 0.05
TH 1000 MgBG	189.4 +/- 12.4	475.0 +/- 10.6	1964.4 +/- 30.9	0.66 +/- 0.03
C57 500 MgO	175.0 +/- 8.2	503.1 +/- 8.8	1843.8 +/- 57.0	0.70 +/- 0.02

Note. * $P < 0.05$ corrected model test - between-subjects' effects. PE % change refers to the extent of the phenylephrine-induced precontractile forces of the femoral arteries prior to the acetylcholine curve measurements. Data represented as mean +/- standard error for $n = 8$ per group. TH 100 MgO (TallyHo, 100mg Mg Oxide/kg chow), TH 500 MgO (TallyHo, 500mg Mg Oxide/kg chow), TH 1000 MgBG (TallyHo, 1000mg Mg Bisglycinate/kg chow), C57 500 MgO (C57BL/6J, 500mg Mg Oxide/kg chow).

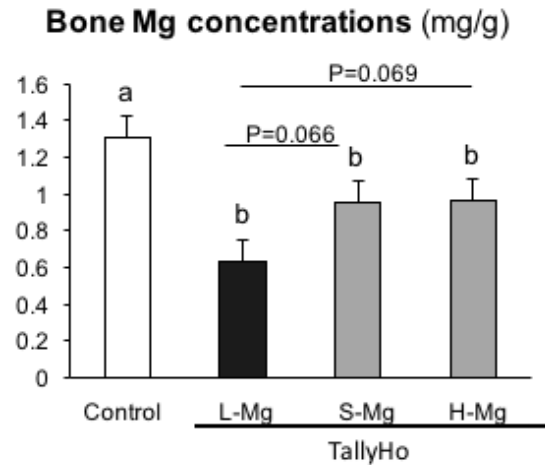


Figure 1. Bone Mg concentrations, measured in milligrams per gram, for the 3 diabetic mouse groups and the control group. Data represented as mean \pm standard error for $n = 8$ per group. Significant difference ($P < 0.05$) is noted using nonsimilar letters. TH L-Mg (TallyHo, 100mg Mg Oxide/kg chow), TH S-Mg (TallyHo, 500mg Mg Oxide/kg chow), TH H-Mg (TallyHo, 1000mg Mg Bisglycinate/kg chow), Control (C57BL/6J, 500mg Mg Oxide/kg chow).

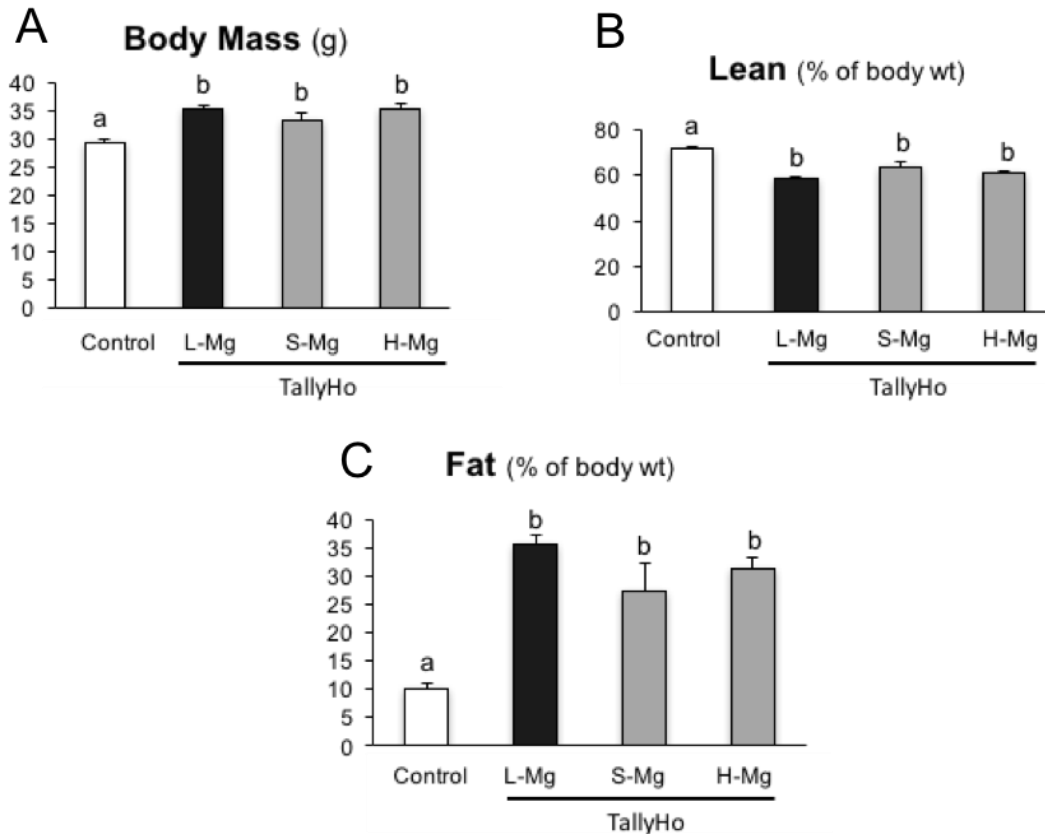


Figure 2. Body composition assessment for the 3 diabetic mouse groups and the control group. (A) Body mass, measured in grams; (B) lean mass, as a percentage of body weight and (C) fat mass, also as a percentage of body weight, for the 3 diabetic mouse groups, and the control group. Data represented as mean \pm standard error for $n = 8$ per group. Significant difference ($P < 0.05$) is noted using nonsimilar letters. TH L-Mg (TallyHo, 100mg Mg Oxide/kg chow), TH S-Mg (TallyHo, 500mg Mg Oxide/kg chow), TH H-Mg (TallyHo, 1000mg Mg Bisglycinate/kg chow), Control (C57BL/6J, 500mg Mg Oxide/kg chow).

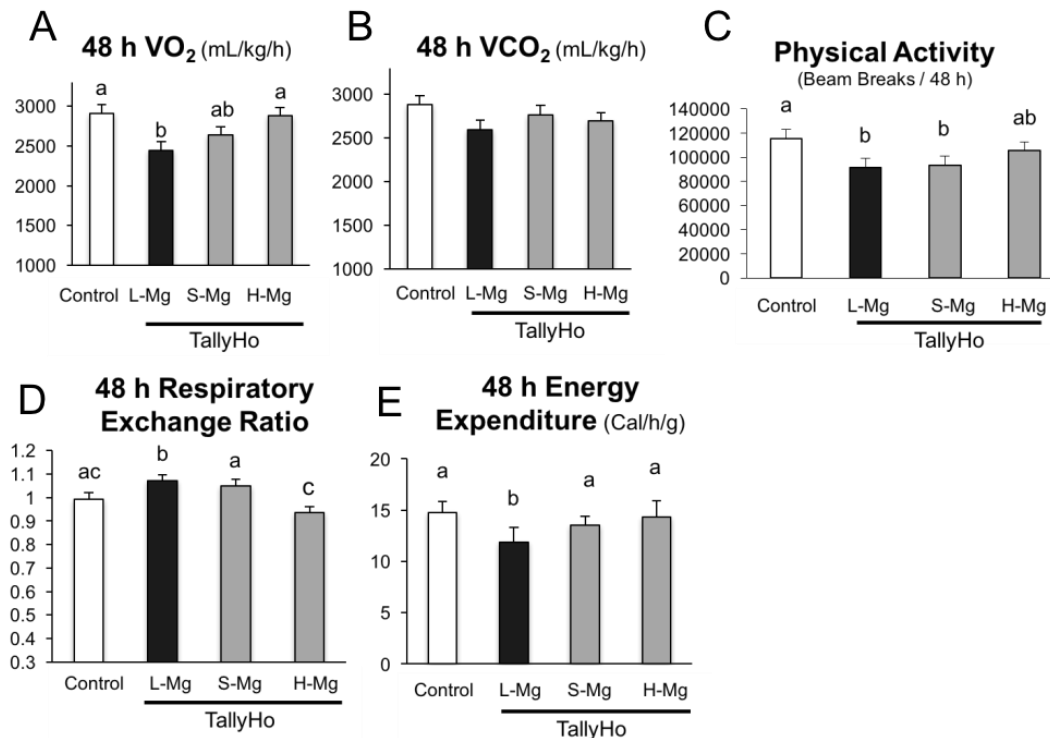


Figure 3. Measurements taken using CLAMS for the 3 diabetic mouse groups and the control group. (A) Volume of oxygen inhaled, measured in milliliters per kilogram body weight per hour; (B) volume of carbon dioxide expired, measured in milliliters per kilogram body weight per hour; (C) physical activity of mice through x, y, and z axis, measured by beam breaks per 48 hours; (D) 48-hour energy expenditure, measured by calories per hour per gram body weight; and (E) 48-hour respiratory exchange ratio. Data represented as mean +/- standard error for $n = 8$ per group. Significant difference ($P < 0.05$) is noted using nonsimilar letters. TH L-Mg (TallyHo, 100mg Mg Oxide/kg chow), TH S-Mg (TallyHo, 500mg Mg Oxide/kg chow), TH H-Mg (TallyHo, 1000mg Mg Bisglycinate/kg chow), Control (C57BL/6J, 500mg Mg Oxide/kg chow).

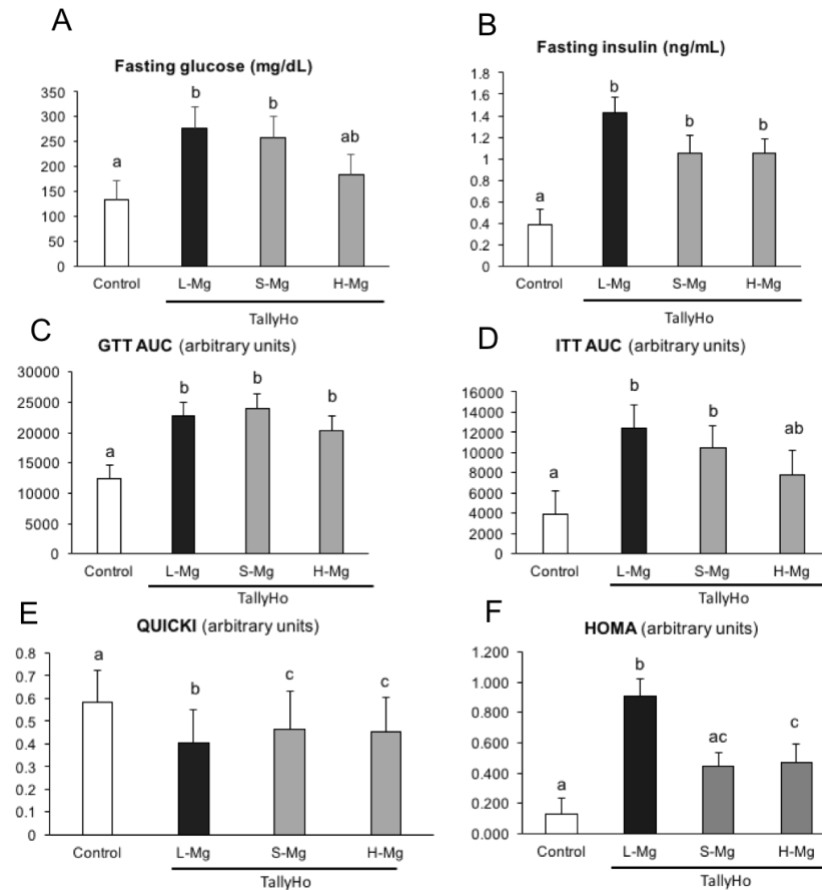


Figure 4. Insulin sensitivity measurements for the 3 diabetic mouse groups and the control group. (A) Fasting serum glucose, measured in milligrams per deciliter; (B) fasting serum insulin, measured in nanograms per deciliter; (C) Insulin Tolerance Test Area Under the Curve; (D) Homeostatic Model Assessment of Insulin Resistance; (E) Quantitative Insulin Sensitivity Check Index; and (F) Glucose Tolerance Test Area Under the Curve. Data represented as mean \pm standard error for $n = 8$ per group. Significant difference ($P < 0.05$) is noted using nonsimilar letters. TH L-Mg (TallyHo, 100mg Mg Oxide/kg chow), TH S-Mg (TallyHo, 500mg Mg Oxide/kg chow), TH H-Mg (TallyHo, 1000mg Mg Bisglycinate/kg chow), Control (C57BL/6J, 500mg Mg Oxide/kg chow).

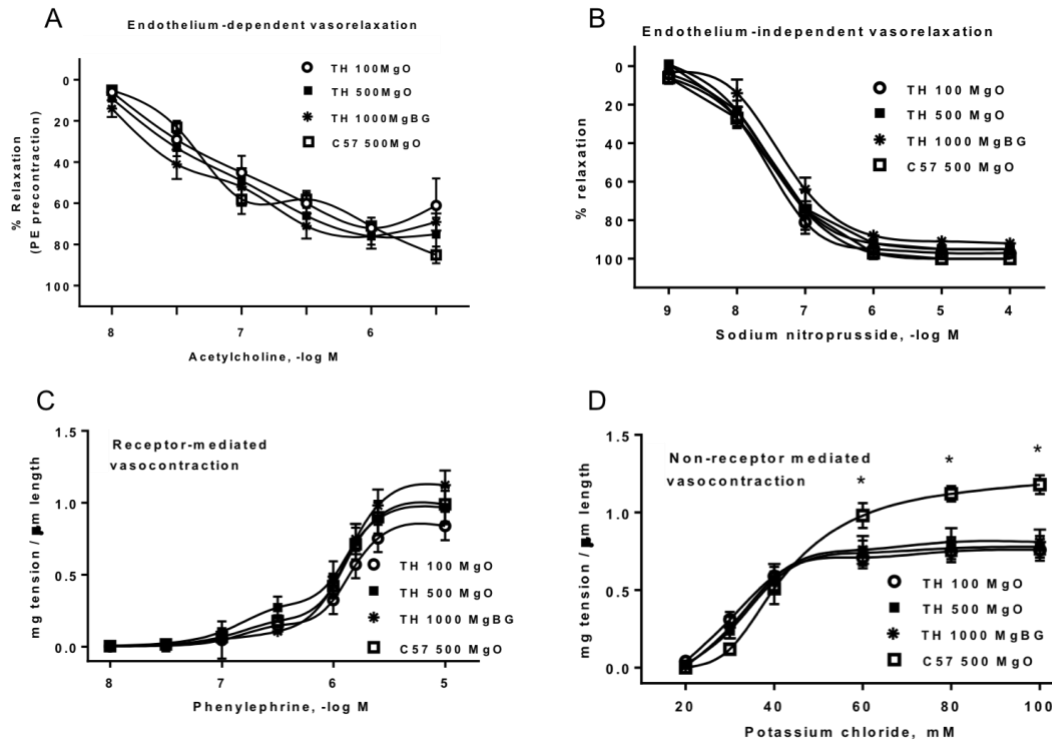


Figure 5. Vessel function curves for the 3 diabetic mouse groups and the control group. (A) Endothelium-dependent vasorelaxation of the femoral artery, using acetylcholine; (B) Endothelium-independent vasorelaxation, using sodium nitroprusside; (C) Receptor-mediated vasoconstriction, using phenylephrine; and (D) Nonreceptor mediated vasoconstriction, using potassium chloride. * $P < 0.05$ vs. Control Mg. Data represented as mean \pm standard error for $n = 8$ per group. TH 100 MgO (TallyHo, 100mg Mg Oxide/kg chow), TH 500 MgO (TallyHo, 500mg Mg Oxide/kg chow), TH 1000 MgBG (TallyHo, 1000mg Mg Bisglycinate/kg chow), C57 500 MgO (C57BL/6J, 500mg Mg Oxide/kg chow).

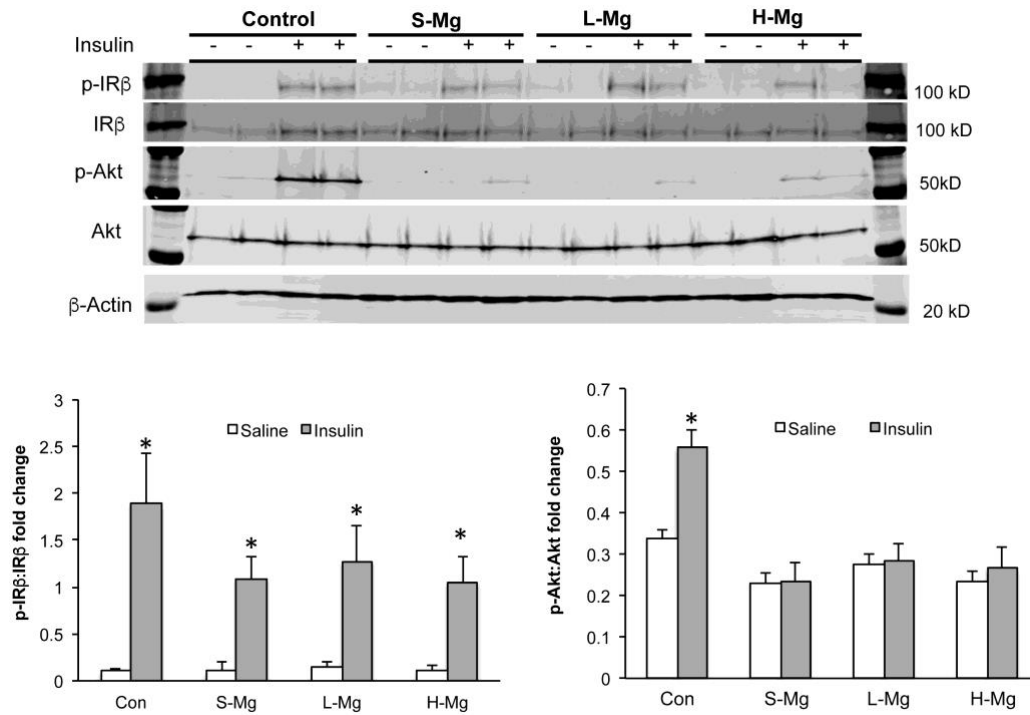


Figure 6. Phospho-Insulin Receptor (p-IR), IR, Phospho-Akt (p-Akt), and Akt concentrations in liver tissue samples between saline and insulin-stimulated mice. $*P < 0.05$ versus saline-treated mice. Data represented as mean \pm standard error for $n = 4$ per group. L-Mg (TallyHo, 100mg Mg Oxide/kg chow), S-Mg (TallyHo, 500mg Mg Oxide/kg chow), H-Mg (TallyHo, 1000mg Mg Bisglycinate/kg chow), Con (C57BL/6J, 500mg Mg Oxide/kg chow).

DISCUSSION

Our study reports for the first time that a low Mg diet fed to TallyHo diabetic mice resulted in reduced energy expenditure, and further exacerbated hyperglycemia and insulin sensitivity. We conclude that a low Mg diet worsens metabolic parameters associated with T2D. Additionally, a high Mg diet of 1000 milligrams Mg per kilogram of chow does not improve diabetic complications in TH mice beyond the level seen in those fed a standard diet.

Type 2 diabetics often exhibit decreased Mg status, due to increased urinary excretion of Mg (15). At reduced plasma concentrations, Mg is rapidly released from the bone. While all TH mice had lower bone Mg content than controls, TH mice fed low Mg diets had significantly lower bone Mg concentrations. Increasing dietary Mg content blunted Mg loss as evidenced by a strong trend toward greater bone Mg for diabetic groups fed the standard and high Mg diets versus those on low Mg diet. Mice fed low Mg may have had increased bone resorption of Mg compared to the other groups. However, a limitation of our study was that we did not measure urine Mg content, and therefore could not confirm that TH mice lost more Mg in their urine.

Mg status does not appear to affect endothelium-dependent or endothelium-independent vessel function, as no significant differences were noted between groups for either mechanism being assessed. Significantly greater nonreceptor mediated contractions were noted in the femoral arteries of the control mice, compared to the TH mice.

Nonreceptor mediated contractions result from potassium chloride stimulation of the femoral arteries. Potassium chloride directly activates voltage-gated calcium channels, causing smooth muscle contraction. Conversely, during receptor-mediated contraction, smooth muscle contraction is initiated by adrenergic alpha-1 receptor, for which phenylephrine is an agonist. Phenylephrine stimulation results in the conversion of phosphatidylinositol (3,4,5)-trisphosphate (PIP₃) to inositol triphosphate (IP₃) and diacylglycerol (DAG). IP₃ is responsible for an increase in cellular calcium, resulting in contraction (16). The significant differences observed between control and TH mice suggests that diabetic phenotypes may worsen nonreceptor mediated contraction of femoral arteries, and that Mg intake does not play a role in the degree of vascular dysfunction observed in this model of diabetes. It has been previously theorized that TallyHo mice exhibit smooth muscle contraction dysfunction, due to oxidative stress and enhanced Rho kinase activity affecting receptor-mediated contraction (17). However, this theory is not applicable to our findings, which saw dysfunction in nonreceptor mediated contraction.

Kobayashi et al. found a strong negative correlation between Mg status and oxygen consumption in human NIDDM subjects (18), but did not report a mechanistic rationale for this relationship. The observation is consistent with our finding that TH mice fed the low Mg diet also had significantly lower oxygen consumption, while TH mice fed adequate Mg were comparable to the control group. The mechanism for this is unclear but there are two possible explanations: i) since oxygen consumption represents physical work capacity (18), diminished oxygen consumption may have been due to a reduction in physical activity; or ii) impaired oxygen delivery to muscle could have reduced the

capacity for physical activity since Mg is required for enzymatic reactions involved in oxygen delivery (19). Both energy expenditure and physical activity, however, did not affect overall body weight of low Mg fed TH mice since body mass of all TH mice were similar and comparable to previously documented weights (20).

Metabolic chamber assessment indicated that TH mice fed the low Mg diet had the highest respiratory exchange ratio (RER), whilst other TH mice were comparable to the control group. A higher RER indicates carbohydrates are the predominant energy source being utilized, whereas a lower RER suggests lipids are the main energy source (21). The RER data however, contrasts with our finding that TH mice fed the low Mg diet had greater insulin resistance and fasting glucose than the other diabetic groups. Theoretically, greater insulin resistance should favor more reliance on lipid oxidation. Given this apparent contradiction, it is possible the reduced oxygen consumption measured in the low Mg fed mice could lead to a higher RER value since RER is calculated as a ratio of volume of oxygen consumed to volume of carbon dioxide produced.

Our general findings regarding fasting insulin and glucose homeostasis are consistent with the previously documented phenotypes of the TallyHo mouse model (20). Kim et al. found TH mice to have impaired glucose tolerance and hyperinsulinemia by 8-weeks of age and postulated that the presence of both glucose intolerance and hyperinsulinemia in TH mice results from a compensatory hypersecretion mechanism, due to diminished peripheral insulin action (20). Our data also demonstrate that dietary Mg may influence the TH phenotype. For example, we found that fasting glucose was highest in TH mice fed low and standard Mg, but partially normalized in high Mg fed TH

such that their glucose levels were in between those of controls and the other TH groups. Similarly, indices of both insulin resistance (HOMA) and insulin sensitivity (QUICKI), were improved in TH mice fed high Mg diets versus low Mg diets as well, providing further evidence for the integral role of Mg for normal metabolism.

Our data regarding insulin resistance agrees with previous studies in both animals and humans that associate a low Mg diet with increased likelihood of insulin resistance (15). Currently, there are no proven mechanistic explanations for this association. We hypothesized that low Mg status could directly affect insulin receptor phosphorylation. Crystal structures of the insulin receptor have shown two Mg ions bind to the tyrosine kinase domain, in order to increase tyrosine kinase affinity for ATP molecules, thus improving kinase activity (22). In previous studies, mice exhibiting hypomagnesemia were found to have reduced levels of phosphorylated insulin receptor in both cardiac and skeletal muscle tissue, giving rise to an insulin resistant phenotype (22). While the aforementioned research supports the idea that hypomagnesemia may worsen insulin resistance in TH mice, molecular evidence from our study found no alteration at the level of the insulin receptor in liver. Specifically, we observed that insulin-stimulated phosphorylation of the insulin receptor in the liver was similar across all control and TH groups. In contrast to the lack of change in hepatic insulin receptor, insulin-stimulated p-Akt : Akt was significantly blunted in all diabetic TH mice versus control mice. However, similarity of p-Akt : Akt in the liver did not reflect the fact that low Mg-fed TH mice have greater whole body insulin resistance compared to high Mg-fed TH mice according to HOMA-IR and QUICKI. Given this paradox, it is possible that other tissues such as skeletal muscle may have changes in insulin-stimulated signaling under high

dietary Mg conditions that could account for the whole body differences reflected in the fasting glucose levels and QUICKI/HOMA-IR indices. On-going studies are testing this hypothesis.

In conclusion, TH mice fed a low Mg diet resulted in reduced energy expenditure, and further exacerbated insulin resistance, and hyperglycemia. The possible molecular culprits for exacerbated insulin resistance in hypomagnesemic TH mice warrant further exploration. These findings also have clinical implications. Mean US adult Mg intake is suboptimal (15). Additionally, diabetic patients are already susceptible to low Mg status (1). Chutia and Lynrah observed serum Mg decreases with increased insulin resistance in T2D patients (4), while Mooren found Mg intake is significantly inversely associated with the risk of T2D in a dose-dependent manner (8). Evidence from our study leads us to speculate that diabetic individuals with low Mg intake may be worsening their condition. While our data did not clearly indicate that a high Mg diet provides a beneficial effect on diabetic vascular complications, we did find evidence that the level of dietary Mg can positively impact various parameters of insulin function. Data from our study supports the concept of Mg supplementation in both prediabetic and diabetic individuals, which should be tested in large scale clinical studies.

REFERENCES

1. Barbagallo M, Dominguez LJ. Magnesium metabolism in type 2 diabetes mellitus, metabolic syndrome and insulin resistance. *Arch. Biochem. Biophys.* 2007;458:40-7.
2. Nelson DL, Cox MM. *Lehninger Principles of Biochemistry*. WH Freeman and Company; 2008.
3. Ford ES, Mokdad AH. Dietary magnesium intake in a national sample of US adults. *J. Nutr.* 2003;133(9):2879-82.
4. Chutia H, Lynrah KG. Association of serum magnesium deficiency with insulin resistance in type 2 diabetes mellitus. *J Lab Physicians.* 2015;7(2):75-8.
5. Chaudhary DP, Sharma R, Bansal DD. Implications of magnesium deficiency in type 2 diabetes: a review. *Biol Trace Elem Res.* 2010;134(2):119-29.
6. Dong JY, Xun P, He K, Qin LQ. Magnesium intake and risk of type 2 diabetes: meta-analysis of prospective cohort studies. *Diabetes Care.* 2011;34(9):2116-22.
7. Solati M, Ouspid E, Hosseini S, Soltani N, Keshavarz M, Dehghani M. Oral magnesium supplementation in type II diabetic patients. *Med J Islam Repub Iran.* 2014;28:67.
8. Mooren FC. Magnesium and disturbances in carbohydrate metabolism. *Diabetes Obes. Metab.* 2015;17:813-823.
9. Balon TW, Gu JL, Tokuyama Y, Jasman AP, Nadler JL. Magnesium supplementation reduces development of diabetes in a rat model of spontaneous NIDDM. *Am J Physiol.* 1995;269:745-752.
10. TALLYHO/JNGJ: A polygenic mouse model of type 2 diabetes [Internet]. The Jackson Laboratory. [Published Oct 1st 2008. Accessed Apr 13th 2016.] Available from <https://www.jax.org/news-and-insights/2008/october/tallyho-jngj-a-polygenic-mouse-model-of-type-2-diabetes>.
11. Boudina S, Sena S, Sloan C, Tebbi A, Han YH, O'Neill BT, Cooksey RC, Jones D, Holland WL, McClain DA, et al. Early mitochondrial adaptations in skeletal

muscle to diet-induced obesity are strain dependent and determine oxidative stress and energy expenditure but not insulin sensitivity. *Endocrinology*. 2012;156(6):2677-2688.

12. Matthews DR, Hosker JP, Rudenski AS, Naylor BA, Treacher DF, Turner RC. Homeostasis model assessment: insulin resistance and beta-cell function from fasting plasma glucose and insulin concentrations in man. *Diabetologia*. 1985;28(7):412-9.
13. Katz A, Nambi SS, Mather K, Baron AD, Follmann DA, Sullivan G, Quon MJ. Quantitative insulin sensitivity check index: a simple, accurate method for assessing insulin sensitivity in humans. *J Clin Endocrinol Metab*. 2000;85(7):2402-10.
14. Park SY, Rossman MJ, Gifford JR, Bharath LP, Bauersachs J, Richardson RS, Abel ED, Symons JD, Riehle C. Exercise training improves vascular mitochondrial function. *Am J Physiol Heart Circ Physiol*. 2016;310(7):821-829.
15. Barbagallo M, Dominguez LJ. Magnesium and type 2 diabetes. *World J Diabetes*. 2015;6(10):1152-1157.
16. Gonzales RJ, Carter RW, Kanagy NL. Laboratory demonstration of vascular smooth muscle function using rat aortic ring segments. *Adv Physiol Educ*. 2000;24(1):13-21.
17. Didion SP, Lynch CM, Faraci FM. Cerebral vascular dysfunction in TallyHo mice: a new model of Type II diabetes. *Am J Physiol Heart Circ Physiol*. 2007;292(3):1579-83.
18. Kobayashi T. Plasma and erythrocyte magnesium levels are correlated with oxygen uptake in patients with non-insulin dependent diabetes mellitus. *Endocr J*. 1998;45(2):277-83.
19. Lukaski HC, Bolonchuk WW, Klevay LM, Milne DB, Sandstead HH. Maximal oxygen consumption as related to magnesium, copper, and zinc nutriture. *Am J Clin Nutr*. 1983;37(3):407-15.
20. Kim JH, Stewart TP, Soltani-Bejnood M, Wang L, Fortuna JM, Mostafa OA, Moustaid-Moussa N, Shoieb AM, McEntee MF, Wang Y, et al. Phenotypic characterization of polygenic type 2 diabetes in TALLYHO/JngJ mice. *J Endocrinol*. 2006;191(2):437-446.
21. Ramos-Jiménez, A., Hernández-Torres, R. P., Torres-Durán, P. V., Romero-Gonzalez, J., Mascher, D., Posadas-Romero, C., Juárez-Oropeza, M. A. The respiratory exchange ratio is associated with fitness indicators both in trained and untrained men: a possible application for people with reduced exercise tolerance. *Clin Med Circ Respirat Pulm Med*. 2008;2:1-9.

22. Gommers LM, Hoenderop JG, Bindels RJ, de Baaij JH. Hypomagnesemia in type 2 diabetes: a vicious circle? *Diabetes*. 2016;65(1):3-13.